V- and W-band Two-Way Waveguide Splitters Fabricated by Metal Additive Manufacturing

Shane Verploegh, *Student Member, IEEE* and Zoya Popović, *Fellow, IEEE*

***Abstract*—V-band and W-band two-way rectangular waveguide splitters are designed and fabricated using additive manufacturing by direct metal laser sintering of AlSiMg and maraging steel. The designs include a septum and tapers which improve performance but are difficult to achieve using conventional split-block machining. Standard WR-15 and WR-10 waveguide flanges are manufactured together with the waveguides and then alignment pin holes are tapped after printing. Otherwise, no post-processing is applied to the components. Measurements show that the maraging steel has better feature fabrication. The measured return loss is below 20 dB over both bands. The measured coupling ranges from 4 to 6 dB in V band and 5 to 8 dB at W band, between waveguide flanges. The estimated loss increase due to surface roughness ranges from 10.8 dB/m at 62.5 GHz to 33.9 dB/m at 92.5 GHz. Measured asymmetries in the coupled port responses are explained by full-wave simulations of the actual fabricated geometry.**

***Index Terms*—3D printing, additive manufacturing, V-band, W-band, millimeter-wave, direct metal laser sintering (DMLS), selective laser melting (SLM), surface roughness, waveguides, combiner, splitter.**

I. Introduction

Recent interest in additive manufacturing (AM) for microwave and millimeter-wave components is motivated by possible reduction in cost and weight of components, as well as shorter manufacturing times. Additionally, 3D printing allows fabricating geometries that are either much more difficult, or even not possible, to fabricate using traditional split-block machining techniques. Examples are corners and edges that are not rounded by the mill bit, or smooth impedance tapers. AM is especially attractive for higher frequency metallic waveguide components. Conductor additive manufacturing methods are limited, and most of them result in roughness that is considered to be too high to result in low loss at frequencies above V-band.

Examples of reported millimeter-wave passive components fabricated using selective laser melting (SLM) include antennas and couplers covering E,D and H bands using a copper alloy [1], [2]. A good overview of work up to 2015 is given in [3]. More recently, metal coated plastic waveguide has been demonstrated from W and D band in [4] up to WR-1.5 (500-750 GHz) and WR-1 (750-1100 GHz) in [5]. High-order SLM waveguide filters with relatively complex internal geometries have been demonstrated with good performance at Ku band, e.g. [6]. However, feature size limitations and additional loss due to surface roughness have limited performance at higher frequencies. In [7], a comparison is presented between four different metal alloy 3D printed V- and W-band straight waveguide sections and directional couplers, along with a comparison to components fabricated in a metal-coated plastic process.

The work presented here focuses on V- and W-band rectangular waveguide 3-dB splitters manufactured using an aluminum alloy and maraging steel alloy, shown in Fig. 1. The shape of the metal waveguide includes smooth impedance tapers, a narrow septum at the waveguide split junction, and colinear ports, all of which would be difficult to fabricate using standard split-block machining.

II. Waveguide Splitter Design, Manufacturing, and Feature Resolution

The waveguide components are designed using finite-element modeling (HFSS) with measured conductivity data assuming smooth waveguide wall surfaces, as in [7]. Fig. 1 shows a photograph of maraging steel (left) and aluminum alloy (right) fabricated splitters with WR-10 and WR-15 waveguide input and output ports. The flanges are 3-D printed using standards UG-387 for WR-10 and UG-385 for WR-15 (MIL-DTL-392/67E).

The splitter design is not a standard E-plane geometry as in [8], but instead attempts to improve return loss and coupled-port isolation using a septum similar to what is presented in [9] and [10]. Fig. 2a shows the overall geometry. The inherent loss due to surface roughness of AM manufacturing is estimated based on [7] and used in the design to provide

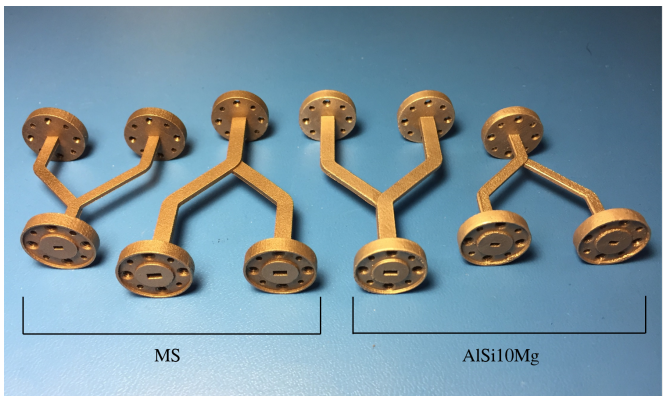

Fig. 1. Photograph of WR-10 and WR-15 waveguide 3-dB splitters implemented in maraging steel (MS) and aluminum alloy ($AlSi_{10}Mg$). The $AlSi_{10}Mg$ components were not functional due to poor printing tolerances that could not meet the dimensions of the internal splitter design geometry.

S. Verploegh and Z. Popović are with the Department of Electrical, Computer, and Energy Engineering, University of Colorado Boulder, Boulder, CO 80309, USA e-mail: (Shane.Verploegh@colorado.edu).

978-1-5386-7333-1/18/$31.00 ©2018 IEEE

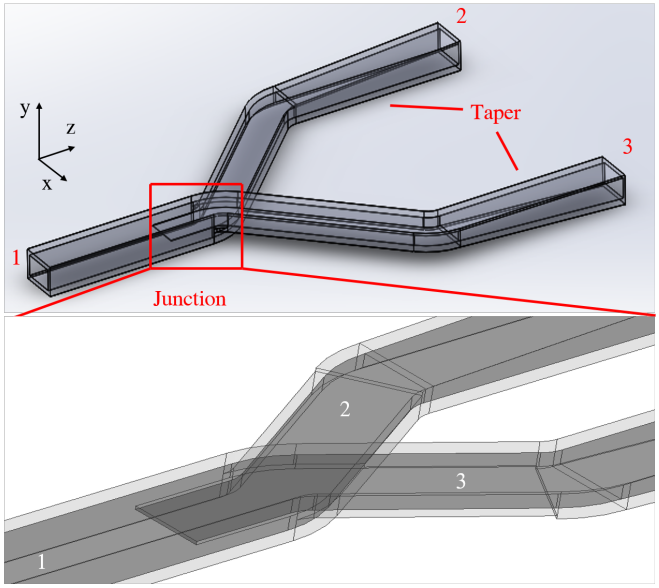

Fig. 2. (a) Transparent 3D-view of the WR-15 waveguide splitter showing continuous tapered impedance waveguide ports 2 and 3. (b) Zoomed-in junction showing septum (width of 0.05 mm) for V band. WR-15 and WR-10 aperture dimensions for designed components are 3.7592 mm × 1.8796 mm and 2.54 mm × 1.27 mm, respectively.

a resistive septum analogous to a Wilkinson divider, shown in detail in Fig. 2b. Instead of a stepped impedance, the work presented here uses a continuous taper enabled by additive manufacturing, indicated in Fig. 2a at waveguide ports 2 and 3. Further, the 3D printing allows output ports (2 and 3) to be colinear with port 1.

The simulated S-parameters of the splitters assuming smooth waveguide walls with loss associated skin depth in maraging steel is shown in Fig. 3, and compared to the performance of a standard E-plane splitter. Notice that the septum and tapered impedance ports contribute to improved input match ($|s_{11}|$) and isolation ($|s_{32}|$). We expect that the measured insertion loss will be increased due to surface roughness.

The components shown in Fig. 1 are fabricated by MidWest Composite Technologies [11], using M270/280 EOS machines with a laser power of 200/400 W, focus of 100 μm and a scan speed of 750 mm/s. The direction of growth is in the $-z$ direction as denoted in Fig. 2. The only post-processing of the components are the center-tapped holes in the flanges.

III. Measurement Results

The components from Fig. 1 are measured with a HP8510C network analyzer with V and W-band extenders (V85104A and W85104A) and waveguide calibration to the flange reference planes. The $AlSi_{10}Mg$ components were not functional due to poor printing tolerances that could not meet the dimensions of the septum and decreased internal height. Figures 4, 5, 6 and 7 show the measured input match, coupling, insertion loss and isolation of the maraging steel components compared to simulations.

Fig. 4 shows the measured input match agrees with the simulations across both bands. In Fig. 5 there is a 2-dB

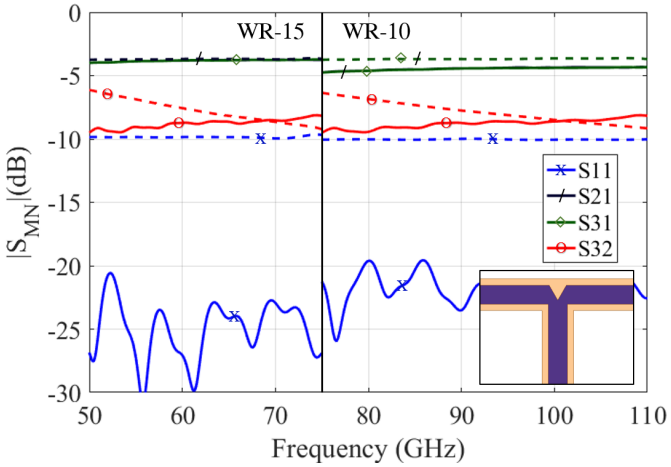

Fig. 3. Simulated S-parameters for the V- and W-band splitters using conductivity of maraging steel [7], $\sigma = 2.05\times10^6$ S/m, and assuming smooth walls. The performance of the splitter geometry from Fig.2 (as solid lines) is compared to a standard E-plane splitter shown in the inset (as dashed lines).

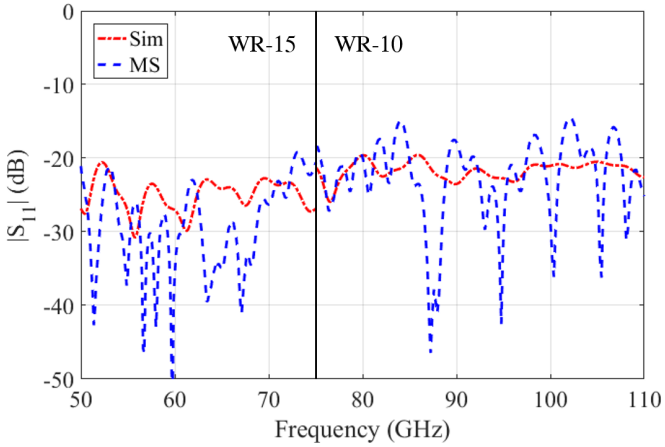

Fig. 4. Simulated (using MS conductivity measured in [7]) and measured reflected power of the WR-10 and WR-15 splitters.

asymmetry between the two ports over the band, which is discussed in the next section. The insertion loss in Fig. 6 is calculated as

$$IL = 20\log\frac{|s_{21}| + |s_{31}|}{\sqrt{2}}$$

The insertion loss is 1.5 dB higher than the predicted value over V-band and 2 dB over W-band. The simulations do not include surface roughness, and the increase in loss is consistent with the results quantified for maraging steel in [7] for the component lengths in Fig.1. The additional loss due to surface roughness, compared to that in Fig. 3 which only takes into account the skin-effect loss, is estimated to be 10.8 dB/m at 62.5 GHz and 33.9 dB/m at 92.5 GHz, consistent with the results in [7]. The isolation between ports 2 and 3 (Fig. 7) shows improved isolation due to increased loss, as expected.

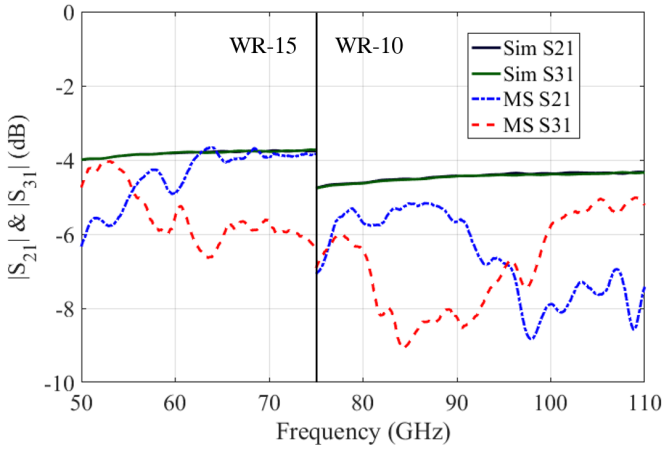

Fig. 5. Simulated (using MS conductivity measured in [7]) and measured power split of the WR-10 and WR-15 splitters.

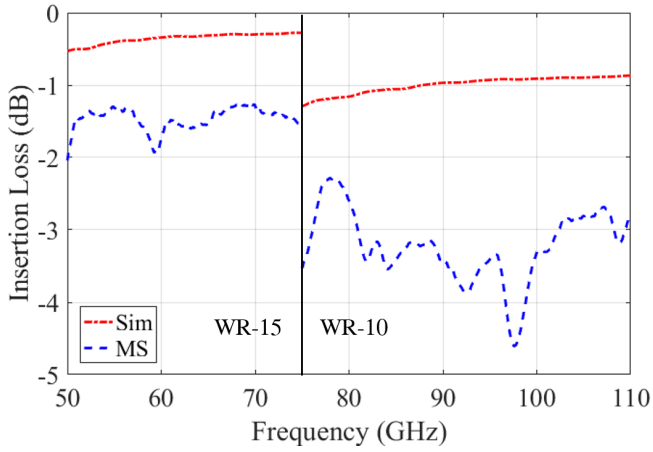

Fig. 6. Simulated (using MS conductivity measured in [7]) and measured insertion loss of the WR-10 and WR-15 splitters.

IV. Fabrication Asymmetry Analysis

The asymmetry in the measured coupling $|s_{21}|$ and $|s_{31}|$ in Fig. 5 is analyzed by first comparing the actual fabricated geometry to the design of the junction shown in Fig. 2b. An optical beam-splitter is used to couple green light into the waveguide port 1, and a camera is focused on the septum portion, resulting in the photo shown in Fig.8. Although it is difficult to focus on all parts of the inner waveguide junction simultaneously, and some parts are not illuminated, it is evident from the photo that the waveguide junction shows a tilt asymmetry in the xy-plane. We believe that the tilt is due to the small dimension of the septum design (50 μm) which is close to twice the particle size of the fabrication process and exhibits a "balling" phenomenon [12]. A similar imperfection was seen in the W-band splitter, with an even larger effect due to more stringent dimensional needs.

From the photograph, the tilt is estimated to be 0.15 mm at the waveguide edge, which corresponds to a 3.9% slope. The geometry shown in the second inset of Fig. 8 is simulated in HFSS and the results are shown in Fig. 9 for the 50-75 GHz band and compared to a perfectly symmetrical junction. Both 1% and 3% slopes result in asymmetry in the coupling, to a varying degree. Although the walls are again assumed to be smooth in the simulation, and the tilt is assumed to be linear, these results explain the measured asymmetry in the coupling coefficients seen in Fig. 5.

V. Conclusion

V-band and W-band two-way rectangular waveguide splitters fabricated using direct laser metal sintering of maraging steel and an aluminum alloy ($AlSi_{10}Mg$) are characterized. The $AlSi_{10}Mg$ components were not functional due to poor printing tolerances that could not meet the dimensions of the septum and decreased internal height. The maraging steel components are characterized and show expected loss since no post-processing is applied after 3D printing. The measured return loss is below 20 dB over both bands. The insertion loss is by 1.5 to 2 dB larger than simulated loss using perfectly smooth waveguide walls, consistent with the roughness characterization in previous work [7].

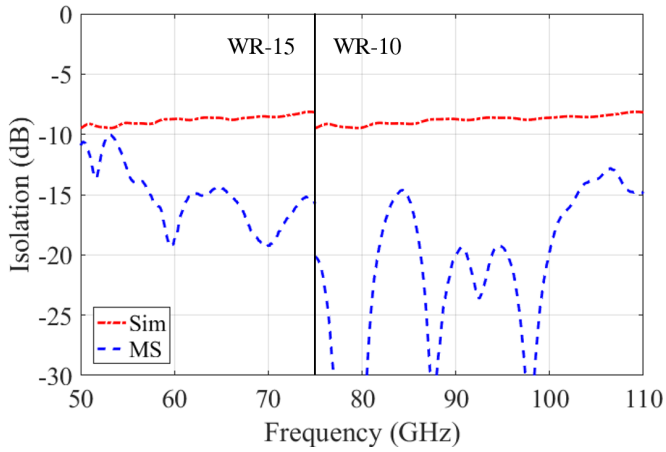

Fig. 7. Simulated (using MS conductivity measured in [7]) and measured isolation between wave-ports 2 and 3 of the WR-10 and WR-15 splitters.

The electromagnetic design pushes the tolerances of the fabrication process to determine its limitations. It is found that the small feature size in the divider junction results in a twisted waveguide wall and full-wave simulations can predict the effect on electrical performance. The junction design includes a 50-μm septum which uses the inherent loss at millimeter-wave frequencies and enables high isolation, but would be difficult to fabricate using standard machining without significant changes in the geometry. The tapers in the coupled-port waveguide sections improve return loss and are included to demonstrate the straightforward capability of 3D printing. All three ports of the divider are colinear; without changing the divider geometry, it is not possible to fabricate this structure with standard machining. Finally, this work shows functional relatively complex waveguide components at millimeter-wave frequencies up to 110 GHz using maraging steel, proving that metal 3D printing is scalable from lower microwave frequencies.

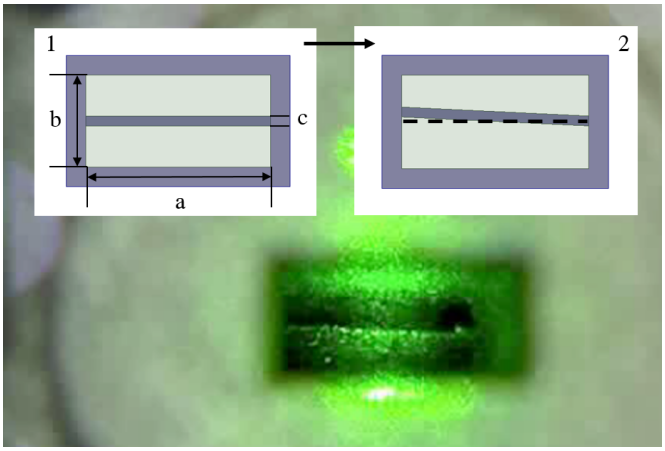

Fig. 8. Photograph of the WR-15 waveguide junction. The dimensions shown in inset 1 are (a) 3.76 mm, (b) 1.88 mm, and (c) 0.05 mm (designed bifurcation width). Inset 2 shows the simulated asymmetry with a linear slope of 3%.

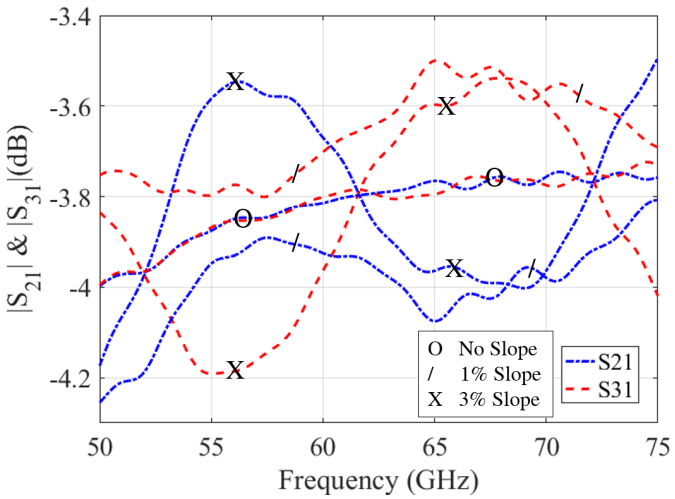

Fig. 9. Simulation of linearly sloped asymmetries in the bifurcation for the WR-15 waveguide splitter compared to the ideal junction geometry (circular symbol. Both 1% (slash symbol) and 3% (cross symbol) show asymmetries similar to the measured coupling coefficients in Fig. 5. The walls of the waveguide are assumed to be perfectly smooth with a conductivity for maraging steel.

ACKNOWLEDGMENT

This work was funded by DARPA under contract number HR001-16-C-0085. The authors would like to thank Dr. Erich Grossman at NIST, Boulder, for useful discussions and for being a great collaborator.

REFERENCES

[1] B. Zhang and H. Zirath, "Metallic 3-D Printed Rectangular Waveguides for Millimeter-Wave Applications," in *IEEE Transactions on Components, Packaging and Manufacturing Technology*, vol. 6, no. 5, pp. 796-804, May 2016.

[2] B. Zhang, Zhaoyao Zhan, Yu Cao, Heiko Gulan, Peter Linner, Jie Sun, Thomas Zwick, and Herbert Zirath, "Metallic 3-D Printed Antennas for Millimeter-and Submillimeter Wave Applications." *IEEE Trans. on Terahertz Science and Tech.*, vol. 6, no. 4, July 2016.

[3] Mario D' Auria, William J. Otter, Jonathan Hazell, Brendan T. Gillatt, Callum Long-Collins, Nick M. Ridler, Stepan Lucyszyn, "3-D Printed Metal-Pipe Rectangular Waveguides." *IEEE Trans. on Components, Packaging and Manufacturing Tech.*, vol. 5, no. 9, Sept 2015.

[4] J. Shen and M. W. Aiken and M. Abbasi and D. P. Parekh and X. Zhao and M. D. Dickey and D. S. Ricketts, "Rapid prototyping of low loss 3D printed waveguides for millimeter-wave applications", *2017 IEEE MTT-S International Microwave Symposium (IMS)* pp. 41-44, June 2017.

[5] W. J. Otter *et al.*, "3D printed 1.1 THz waveguides," in *Electronics Letters*, vol. 53, no. 7, pp. 471-473, Mar. 2017.

[6] O. A. Peverini *et al.*, "Selective Laser Melting Manufacturing of Microwave Waveguide Devices," in *Proceedings of the IEEE*, vol. 105, no. 4, pp. 620-631, Apr. 2017.

[7] S. Verploegh, M. Coffey, E. Grossman and Z. Popovic, "Properties of 50110-GHz Waveguide Components Fabricated by Metal Additive Manufacturing," in *IEEE Transactions on Microwave Theory and Techniques*, vol. 65, no. 12, pp. 5144-5153, Dec. 2017.

[8] R. R. Mansour and J. Dude, "Analysis of microstrip T-junction and its application to the design of transfer switches," *1992 IEEE MTT-S Microwave Symposium Digest*, Albuquerque, NM, USA, pp. 889-892 vol.2, 1992.

[9] L. W. Epp, D. J. Hoppe, A. R. Khan and S. L. Stride, "A High-Power Ka-Band (3136 GHz) Solid-State Amplifier Based on Low-Loss Corporate Waveguide Combining," in *IEEE Transactions on Microwave Theory and Techniques*, vol. 56, no. 8, pp. 1899-1908, Aug. 2008.

[10] F. Takeda, O. lshida and Y. Isoda, "Waveguide Power Divider Using Metallic Septum with Resistive Coupling Slot," *1982 IEEE MTT-S International Microwave Symposium Digest*, Dallas, TX, USA, pp. 527-528, 1982.

[11] https://www.midwestcomposite.com/

[12] P. Hanzl, M. Zetek, T. Baka, and T. Kroupa, "The Influence of Processing Parameters on the Mechanical Properties of SLM Parts", *Procedia Engineering*, vol. 100, pp. 1405-1413, 2015.